Journal of Analytical Science and Technology

RESEARCH ARTICLE Open Access

Multi-isotope signatures (Cu, Zn, Pb) of different particle sizes in road-deposited sediments: a case study from industrial area

Hyeryeong Jeong[1,2] and Kongtae Ra[1,2*]

Abstract

Road-deposited sediments (RDS) are major sources of heavy metal contamination in urban areas and adversely affect surrounding environments and human health. Multi-isotope combinations (Cu, Zn, and Pb), which serve as environmental tracers, enable the identification and management of metal contaminants in RDS. Here, we present Cu, Zn, and Pb isotopic data for the first time in size-fractionated RDS samples collected from industrial areas to describe the relationship between the RDS and total suspended solids (TSS) in runoff, and to explore the feasibility of using multi-isotopes to identify sources of metal contamination. RDS in the industrial study areas had high concentrations of Cu, Zn, and Pb, and their $\delta^{65}Cu_{AE647}$, $\delta^{66}Zn_{IRMM3702}$, and $^{206}Pb/^{207}Pb$ values ranged from −0.33 to +0.73‰, −0.36 to +0.01‰, and 1.1418 to 1.1616, respectively. The variation in $\delta^{65}Cu_{AE647}$ ($\delta^{65}Cu_{max\text{-}min}$) was larger than that of $\delta^{66}Zn_{IRMM3702}$ (i.e., $\delta^{66}Zn_{max\text{-}min}$), and the isotope values of Zn and Pb ($^{206}Pb/^{207}Pb$) tended to increase with the concentrations of these elements. Meanwhile, the fine RDS particles (< 63 μm) had similar Cu, Zn, and Pb isotopic compositions to those of TSS. Hierarchical cluster analyses revealed that the < 63 μm RDS fractions were associated with the TSS. Our results also showed that a combination of Pb and either Cu or Zn could be used to distinguish between RDS and non-exhaust emissions (e.g., brake pads, tires, etc.). Multi-isotope approaches utilizing Cu, Zn, and Pb and more robust isotopic data on individual sources of metal contamination could be useful for identifying pollution sources and understanding their environmental impacts.

Keywords: Cu–Zn–Pb isotopes, Heavy metals, Road-deposited sediments, Industrial land area, Source identification

Introduction

Road surfaces are hot spots for heavy metal pollution because of the accumulation of road-deposited sediments (RDS) via human activities. Road-deposited sediments in urban environments are highly polluted with Cu, Zn, and Pb due to traffic-related activities, such as tire, and brake pad wear and engine emissions (Adamiec et al. 2016; Amato et al. 2011; Iijima et al. 2007; Jeong et al. 2020a; Lanzerstorfer 2020). They are a major source of metal pollution in surrounding atmospheric particles, roadside soils, and stream sediments, as they can be readily transported into aquatic and atmospheric environments by stormwater runoff and resuspension by the wind (Bretón et al. 2019; Jeong et al. 2020b; Khalid et al. 2018; Nawrot et al. 2020; Popoola et al. 2017; Wang and Zhang 2018). Heavy metal concentrations such as Cu, Zn, and Pb in RDS have been used as tracers to identify metal pollution associated with traffic activities, but they are of limited use in discerning the exact source of pollution for each metal (Amato et al. 2009, 2011, 2020c; Bourotte et al. 2019; Hwang et al. 2016; Jeong et al. 2020a).

Many researchers have determined the isotopic compositions of single elements, such as Cu (Little et al. 2017; Song et al. 2016; Wang et al. 2020), Zn (Desaulty et al. 2020; Spinks and Uvarova 2019; Tu et al. 2020), and

*Correspondence: ktra@kiost.ac.kr
[1] Marine Environmental Research Center, Korea Institute of Ocean Science and Technology (KIOST), Busan 49111, Republic of Korea
Full list of author information is available at the end of the article

Springer Open

© The Author(s) 2021. **Open Access** This article is licensed under a Creative Commons Attribution 4.0 International License, which permits use, sharing, adaptation, distribution and reproduction in any medium or format, as long as you give appropriate credit to the original author(s) and the source, provide a link to the Creative Commons licence, and indicate if changes were made. The images or other third party material in this article are included in the article's Creative Commons licence, unless indicated otherwise in a credit line to the material. If material is not included in the article's Creative Commons licence and your intended use is not permitted by statutory regulation or exceeds the permitted use, you will need to obtain permission directly from the copyright holder. To view a copy of this licence, visit http://creativecommons.org/licenses/by/4.0/.

Pb (Gmochowska et al. 2019; Graney et al. 2019; Mil-Homens et al. 2017) during their environmental pollution studies. In a study area with a simple pollution source, it is possible to classify the pollutant source through a single isotope study. Heavy metals in the environment are derived from complex mixtures of natural and anthropogenic sources introduced through various pollution pathways and most environments are contaminated with many metals. In order to overcome the limitations of single elements and to distinguish multiple metal contamination sources, isotopic studies are now being conducted using combinations of two elements, namely Cu and Pb (Jeong et al. 2020b; Mihaljevič et al. 2019), Cu and Zn (Araújo et al. 2019a; Novak et al. 2016), and Zn and Pb (Rosca et al. 2019). Determining multi-elements isotopic compositions of Cu, Zn, and Pb can be a powerful tool for more accurate identification of various sources of pollution. For example, multi-isotope approaches have been applied to identify and discriminate among individual metal sources in urban aerosols (Souto-Oliveira et al. 2018, 2019; Schleicher et al. 2020) and coastal sediments (Araújo et al. 2019b).

Heavy metals in RDS occur at higher concentrations in finer particles, and these size fractions account for a higher proportion of all RDS (Jeong et al. 2020d; Zhao et al. 2010). Because the particle size distribution of RDS is closely related to particle mobility (Amato et al. 2012; Li et al. 2016), a consideration of particle size is needed to trace metal pollutants more clearly and to understand their associated pollution pathways. In this study, we aim to understand the variations in the Cu, Zn, and Pb isotopic compositions of different RDS particle sizes, as well as the relationship between RDS and total suspended solids (TSS) in runoff. We also consider whether multi-isotope studies wherein Cu, Zn, and Pb are combined can provide meaningful insights into the sources of metal pollution in the RDS of industrial regions.

Material and methods

Study area and sample collection

The Shihwa National Industrial Complex in Ansan, South Korea, has 18,612 small-scale facilities in operation. According to our previous study, Siheung Stream showed the highest pollution levels of Cu (10,977 mg/kg), Zn (3875 mg/kg), and Pb (2669 mg/kg) among the five streams flowing through this industrial complex (Jeong et al. 2019). These metals caused by industrial activities transport to stream and coastal environments via atmospheric deposition or rainfall runoff. In the study area, there is a significant level of metal contamination nearby the industrial area. This suggests that the influence of rainfall runoff is greater than atmospheric deposition. Therefore, we selected a small upstream catchment area of Siheung Stream as the study area. A total of 37 industrial facilities operates over a drainage area of 0.166 km^2 (Fig. 1). As copper smelting and refining facilities are present here, cable manufacturing and nonferrous and primary metal manufacturing industries where Cu is used are also active and account for 70% of all industries in the study area.

Sampling the RDS and TSS in runoff was conducted in May 2018. Road-deposited sediments were collected from 11 sites at equal intervals using a Dyson vacuum cleaner (DC-35, Dyson Ltd., UK). Four subsamples were taken per site to ensure that sampling was representative. Before RDS sampling, the vacuum cleaner was disassembled and cleaned to prevent cross-contamination. After removing the coarse RDS particles (> 2 mm), the RDS samples were divided into six different size fractions (> 1000, 500–1000, 250–500, 125–250, 63–125, and < 63 μm) using automatic sieves (Analysette 3, Fritsch Co., Germany) in accordance with Wentworth (1992). Total suspended solid sampling was also conducted for a rainfall event that had a 5-day antecedent dry period (total rainfall = 10.9 mm). Twelve of the TSS samples were collected during a 17-h period and were separated using an acid-cleaned, 0.4 μm polycarbonate filter (47 mm diameter, Whatman, MilliporeSigma, USA) in a Class 1000 clean room.

Heavy metal analysis

The size-fractionated RDS samples were weighed after oven drying at 60 °C and pulverized using an automatic grinding machine (Pulverisette 6, Fritsch Co., Germany). Homogenized RDS and TSS samples were digested with high-purity mixed acids (fluoric, hydrochloric, and perchloric) on a hot plate. Seven metals (Cr, Ni, Cu, Zn, As, Cd, and Pb) were then analyzed via inductively coupled plasma mass spectrometry (ICP-MS; iCAP Q, Thermo Fisher Scientific, Germany) at the Korea Institute of Ocean Science and Technology (KIOST). Certified reference materials were also analyzed to ensure the quality of our metal analyses. The recoveries of two types of certified reference materials (MESS-4 and PACS-3 from the National Research Council Canada) ranged from 92.0% (Ni) to 99.7% (Pb) for MESS-4 and 90.9% (Pb) to 103.7% (Cr) for PACS-3.

Cu, Zn, and Pb isotopes analysis

For Cu and Zn isotopic analyses, these elements were separated from matrix elements, such as Na, Mg, Ca, Ti, Cr, Fe, and Ba, using an anion exchange resin (AG-MP1, Bio-Rad Laboratories, Inc., USA) (Jeong et al. 2021). The Pb in RDS and TSS samples was separated from

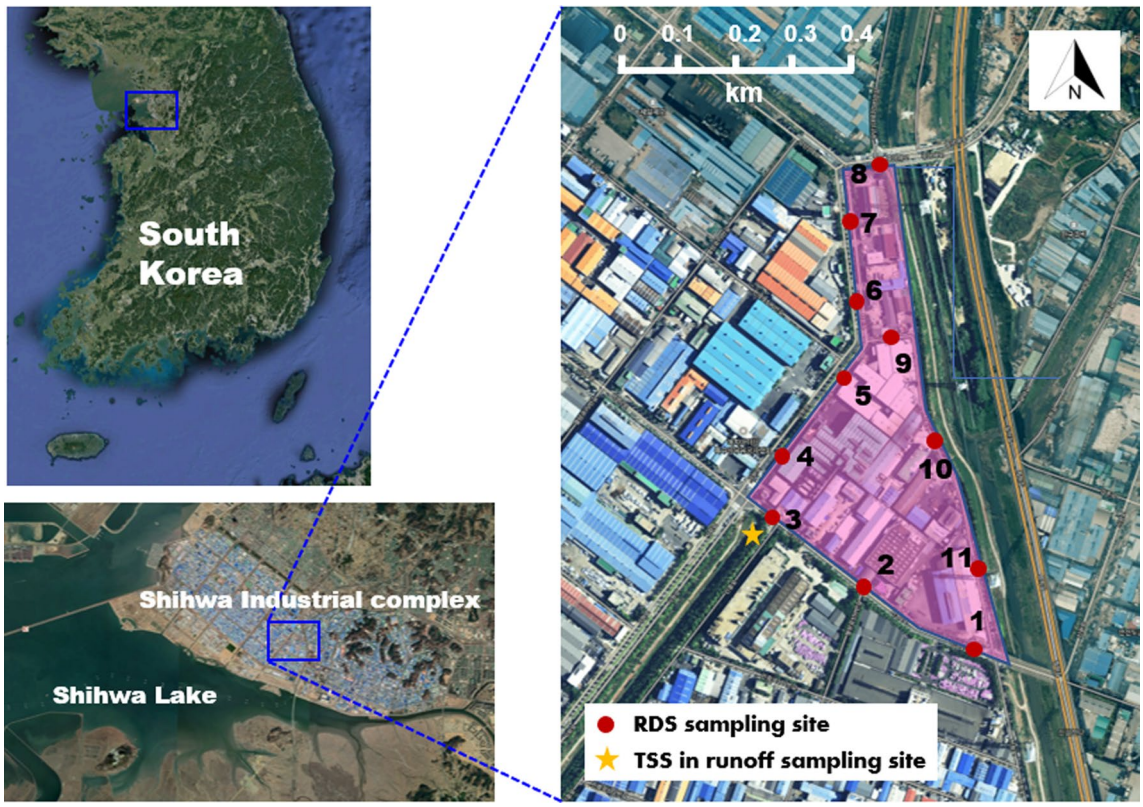

Fig. 1 Study area and sampling sites of RDS and TSS in rainfall runoff at industrial complex of Korea (The purple area represents the drainage area for runoff, base map from Google Earth)

interference elements using a Pb-specific resin (Eichrom Technologies, Inc., USA). The detailed chemical procedures and isotopic analyses were reported in our previous study (Jeong et al. 2021).

Isotopic measurements were performed using a Neptune Plus multicollector-ICP-MS (Thermo Fisher Scientific, Germany) at the KIOST. A mass-bias correction was performed via the standard sample bracketing (SSB) method, using the measurements of ERM-AE647 for Cu, IRMM-3702 for Zn, and NIST SRM 981 for Pb. Purified Cu, Zn, and Pb concentrations were matched to less than ± 5% to yield precise isotopic measurements. The Cu and Zn isotopic data are expressed in delta (δ) notation as permil (‰) deviations from the isotopic standards (ERM-AE647 and IRMM-3702, respectively) as follows:

$$\delta^{65}\mathrm{Cu}(‰) = \left(\frac{\left(^{65}\mathrm{Cu}/^{63}\mathrm{Cu}\right)_{\mathrm{sample}}}{\left(^{65}\mathrm{Cu}/^{63}\mathrm{Cu}\right)_{\mathrm{ERM\,-\,AE647}}} - 1 \right) \times 1000 \quad (1)$$

$$\delta^{66}\mathrm{Zn}(‰) = \left(\frac{\left(^{66}\mathrm{Zn}/^{64}\mathrm{Zn}\right)_{\mathrm{sample}}}{\left(^{66}\mathrm{Zn}/^{64}\mathrm{Zn}\right)_{\mathrm{IRMM\,-\,3702}}} - 1 \right) \times 1000 \quad (2)$$

For comparison with our results, previously reported Cu and Zn isotopic data were converted from SRM 976 to ERM-AE647 and JMC-Lyon to IRMM-3702 (Moeller et al. 2012; Araújo et al. 2017), respectively (Eqs. 3 and 4).

$$\delta^{65}\mathrm{Cu}_{\mathrm{ERM\,-\,AE647}} = \delta^{65}\mathrm{Cu}_{\mathrm{NIST\ 976}} - 0.21‰ \quad (3)$$

$$\delta^{66}\mathrm{Zn}_{\mathrm{IRMM\,-\,3702}} = \delta^{66}\mathrm{Zn}_{\mathrm{JMC}} - 0.27‰ \quad (4)$$

The repeatability and bias for Cu and Zn were obtained by measuring ERM-AE647 (0.00 ± 0.02‰, 2 s, $N = 8$) and IRMM-3702 (0.00 ± 0.01‰, 2 s, $N = 7$). The average analytical uncertainty (2 s) of sample measurements using SSB method yielded between ± 0.01‰ and ± 0.04‰ for $\delta^{65}\mathrm{Cu}_{\mathrm{AE647}}$ and $\delta^{66}\mathrm{Zn}_{\mathrm{IRMM3702}}$.

Heavy metal loadings on a grain size fraction

Grain size fraction loadings ($\mathrm{GSF}_{\mathrm{loading}}$) were determined by calculating the metal loading ratios of the six grain size fractions of RDS, and $\mathrm{GSF}_{\mathrm{loading}}$ was expressed as follows:

$$GSF_{loading} = 100 \times \left[\frac{X_i \times GS_i}{\sum_{i=1}^{6} X_i \times GS_i} \right]. \quad (5)$$

where X_i is the metal concentration in each particle size fraction and GS_i is the percentage of the total mass of the sample accounted for by each size fraction. The total $GSF_{loading}$ is 100% (Sutherland 2003).

Results and discussion

Heavy metal concentrations in different RDS size fractions and TSS

Mean metal concentrations of RDS are shown in Table 1. The Cu concentration was significantly higher than those of the other metals owing to the copper smelting facilities concentrated in the area. We found that the mean concentrations of Cu in RDS were in the following order by particle size: below 63 μm (20,089 mg/kg) > 63–125 μm (8245 mg/kg) > 125–250 μm (4056 mg/kg) > 250–500 μm (2340 mg/kg) > 500–1000 μm (1273 mg/kg) > above 1000 μm (353 mg/kg). Zn concentrations of 250–500 μm, 125–250 μm, and 63–125 μm fractions were higher than other urban RDS (Jeong et al. 2020e; Zafra et al. 2011). Additionally, Zn concentration of < 63 μm fraction was similar to another industrial RDS in Korea (Jeong et al. 2020f) and Zn concentration of TSS in this study was 3 to 16 times higher than other urban and industrial roads (Table 1). Mean Pb concentration of < 63 μm fraction (5797 mg/kg) was 2 times higher than TSS in this study and was 16 to 28 times higher than urban/industrial regions (Table 1). Other metal concentrations (Cr, Ni, Zn, As, Cd, and Pb) also tended to increase in smaller particle sizes. However, Li showed no difference in concentrations according to the RDS sizes, indicating that the metal concentrations in the RDS were significantly affected by anthropogenic sources. In the fine RDS (< 63 μm), the mean metal concentrations in descending order were: Cu (20,089 mg/kg) > Pb (5797 mg/kg) > Zn (2541 mg/kg) > Cr (1488 mg/kg) > Ni (638 mg/kg) > As (28.5 mg/kg) > Cd (10.2 mg/kg) (Fig. 2).

The mean concentrations of heavy metals in TSS samples are as follows: Cu (16,294 mg/kg), Zn (9921 mg/kg), Pb (2391 mg/kg), Cr (737 mg/kg), Ni (436 mg/kg), Cd (50.2 mg/kg), and As (26.1 mg/kg) (Table 2). Zn and Cd in TSS samples showed higher concentrations than the finest particles (< 63 μm) in RDS. The mean concentrations of other metals showed values similar to < 125 μm, but showed higher value than that of particles over

Table 1 Means and standard deviations (1 s) of heavy metal concentrations in six different particle sizes of RDS and TSS in runoff in this study

Particle size	Li	Cr	Ni	Cu	Zn	As	Cd	Pb
μm	mg/kg	mg/kg	mg/kg	mg/kg	mg/kg	mg/kg	mg/kg	mg/kg
> 1000	16.9 ± 3.7 (12.3–26.0)	110 ± 83 (42–292)	22 ± 6 (15–36)	353 ± 380 (81–1326)	261 ± 131 (119–524)	7.2 ± 6.0 (3.4–23.1)	0.7 ± 0.4 (0.2–1.5)	214 ± 128 (71–445)
500–1000	15.4 ± 1.6 (13.0–18.4)	223 ± 192 (69–614)	139 ± 311 (18–1072)	1273 ± 2539 (159–8828)	477 ± 183 (230–722)	9.7 ± 3.2 (6.3–16.9)	1.1 ± 0.7 (0.5–2.7)	448 ± 359 (130–1423)
250–500	13.7 ± 1.3 (11.8–15.8)	393 ± 255 (108–917)	87 ± 103 (22–349)	2340 ± 2511 (308–8081)	1089 ± 965 (356–3341)	13.4 ± 7.1 (5.9–31.8)	1.5 ± 0.9 (0.6–2.8)	974 ± 1413 (210–5094)
125–250	14.0 ± 1.6 (11.2–16.0)	691 ± 580 (154–2159)	238 ± 258 (46–945)	4056 ± 4851 (648–17,681)	1360 ± 793 (671–2973)	14.6 ± 4.3 (9.2–22.2)	2.9 ± 1.2 (1.5–4.9)	1342 ± 970 (378–3010)
63–125	15.4 ± 1.6 (11.2–17.6)	1094 ± 1263 (414–4829)	469 ± 655 (130–2408)	8245 ± 10,684 (1064–37,301)	1891 ± 646 (1175–2877)	15.4 ± 3.4 (10.3–22.9)	4.4 ± 2.4 (2.2–10.6)	2140 ± 1539 (682–4409)
< 63	19.8 ± 2.0 (17.6–22.8)	1488 ± 1180 (434–4527)	638 ± 534 (210–2068)	20,089 ± 25,406 (4367–81,262)	2541 ± 587 (1797–3627)	28.5 ± 7.7 (15.4–38.0)	10.2 ± 3.3 (4.5–16.6)	5797 ± 3417 (1955–11,169)
TSS	23.2 ± 12.7 (2.0–37.9)	737 ± 501 (69–1445)	436 ± 528 (128–2006)	16,294 ± 8167 (1747–27,631)	9921 ± 4159 (3680–16,537)	26.1 ± 10.6 (6.2–39.3)	50.2 ± 23.5 (16.9–94.7)	2391 ± 1075 (156–3848)
Urban Road (Ansan) < 63[a]	15.8	167	50.3	160	907	15.7	1.4	207
Urban road (Spain) < 63[b]	–	–	–	124	630	–	38	350
Industrial road (Gwangyang) < 63[c]	–	841	246	193	2982	16.0	2.1	221

[a] Jeong et al. (2020e)

[b] Zafra et al. (2011)

[c] Jeong et al. (2020f)

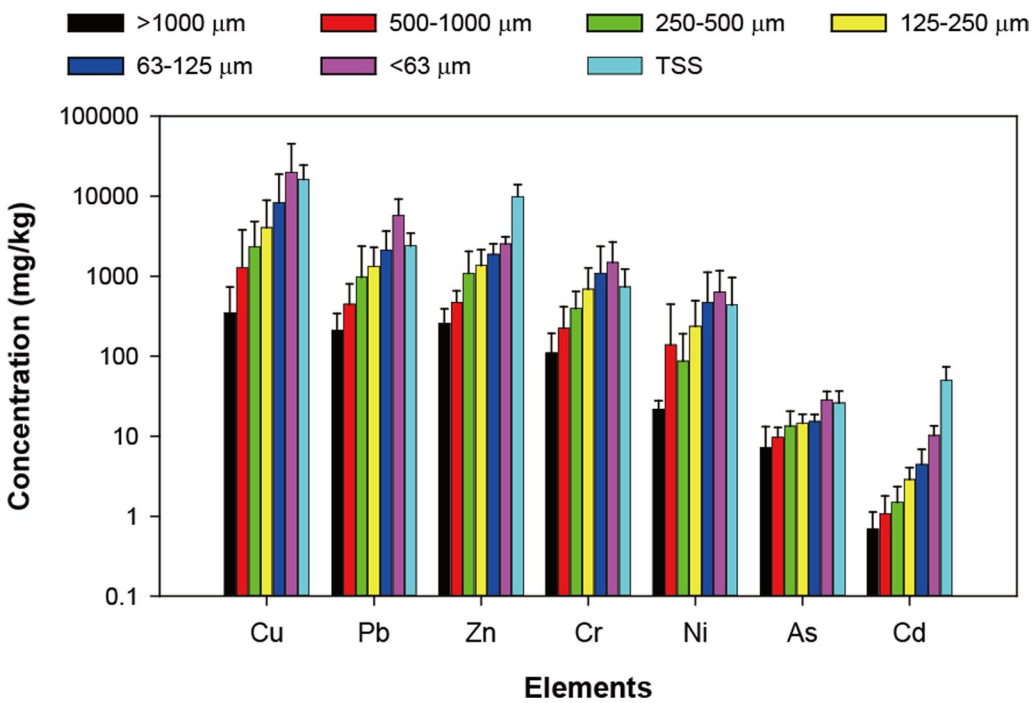

Fig. 2 Comparison of heavy metal concentrations in different sizes of RDS and TSS in this study

Table 2 Comparison of mean, minimum, and maximum values for Cu, Zn, and Pb isotopic composition of this study and other reported literature data

Particle size (μm)	$\delta^{65}Cu_{AE647}$(‰)	$\delta^{66}Zn_{IRMM3702}$(‰)	$^{206}Pb/^{207}Pb$	References
> 1000	− 0.01 (− 0.23 to 0.23)	− 0.21 (− 0.36 to − 0.12)	1.1500 (1.1418–1.1561)	This study (*N* = 11)
500–1000	0.08 (− 0.08 to 0.51)	− 0.19 (− 0.30 to − 0.10)	1.1537 (1.1495–1.1556)	This study (*N* = 11)
250–500	− 0.08 (− 0.33 to 0.12)	− 0.17 (− 0.22 to − 0.06)	1.1540 (1.1488–1.1610)	This study (*N* = 11)
125–250	0.10 (− 0.07 to 0.73)	− 0.18 (− 0.25 to − 0.06)	1.1536 (1.1476–1.1570)	This study (*N* = 11)
63–125	0.03 (− 0.07 to 0.09)	− 0.20 (− 0.26 to − 0.12)	1.1545 (1.1499–1.1616)	This study (*N* = 11)
< 63	0.03 (− 0.13 to 0.16)	− 0.13 (− 0.27 to 0.01)	1.1568 (1.1539–1.1596)	This study (*N* = 11)
TSS	0.01 (− 0.11 to 0.15)	− 0.11 (− 0.21 to − 0.02)	1.1534 (1.1516–1.1554)	This study (*N* = 12)
Road dust (São Paulo)	− 0.07 (− 0.13 to 0.4)	− 0.15 (− 0.19 to 0.10)	1.1740 (1.1600–1.1860)	(Souto-Oliveira et al. 2018) (*N* = 5)
Road paint (UK)	0.03 (− 0.39 to 0.35)	0.10 (− 0.20 to 0.31)	1.1577 (1.1471–1.1708)	(Dong et al. 2017) (*N* = 4)
Brake (UK)	0.30 (0.07–0.42)	− 0.10 (− 0.12 to − 0.07)	1.2133 (1.1651–1.2547)	(Dong et al. 2017) (*N* = 3)
Tire (UK)	0.05 (− 0.04 to 0.12)	− 0.07 (− 0.08 to − 0.06)	1.1607 (1.1502–1.1660)	(Dong et al. 2017) (*N* = 3)

125 μm. After the beginning of precipitation, the concentration of TSS increased by 13.6 times for Li, 10.1 times for Cu, 17.3 times for Pb, 3.0 times for Zn, 12.1 times for Cr, 4.7 times for As, and 3.2 times for Cd. These results suggest that the fine particles accumulated on the road surface were discharged by rainfall runoff. There are

copper smelter and refinery in this study area, and copper alloy manufacturers (generator, copper wire, and cable manufacturer) are concentrated in the vicinity. The Cu concentrations in this industrial region were more than 100 times higher than urban/industrial RDS elsewhere in South Korea (Jeong et al. 2020e, f) and Spain (Zafra et al. 2011) (Table 1), and the mean concentration of Cu was higher than the maximum (8980 mg/kg) in highly contaminated soils near the Mufulira copper smelter in Zambia (Konečný et al. 2014). Due to the influence of Cu smelting facilities and Cu alloy processing industries, the Cu concentration was extremely high compared to urban RDS (mean of 370 mg/kg, Jeong et al. 2020a), but Cr, Ni, Cd, and Pb were also higher than urban RDS. Cr and Ni showed the highest concentrations of RDS of most particle sizes at sampling site 3, where copper smelting and refinery are concentrated. Our previous study reported that RDS around the paper and cardboard manufacturing industry were highly contaminated with Cr (2565 mg/kg), Pb (2263 mg/kg), and Cd (20.9 mg/kg) (Jeong et al. 2020d). There are also manufacturers of corrugated cardboard and paper in this study area and various industrial facilities exist. Therefore, the metal contamination of the RDS in this study area may be affected not only by copper smelting and processing activities, but also by various industrial and traffic activities.

Cu isotopic compositions of different RDS size fractions

The $\delta^{65}Cu_{AE647}$ values of the different RDS size fractions are shown in Table 2. The Cu isotopic composition ranged from −0.33 to +0.73‰, and the mean $\delta^{65}Cu_{AE647}$ values were −0.01‰ (>1000 μm), +0.08‰ (500–1000 μm), −0.08‰ (250–500 μm), +0.10‰ (125–250 μm), +0.03‰ (63–125 μm), and +0.03‰ (<63 μm) (Table 2). Figure 3a illustrates the relationship between $\delta^{65}Cu_{AE647}$ and its concentration in the different RDS size fractions. No correlation was found between $\delta^{65}Cu_{AE647}$ and its concentration.

Variation of Cu isotopic composition (~1.05‰) was greater than Zn isotopic composition (~0.37‰) in this study. In case of Cu isotopes, there were large variations in low temperature environments (~5.86‰) and various natural materials (~36.53‰) (Wang et al. 2017). Redox reaction, adsorption, complexation with organic matters/minerals, and biological process can affect the Cu isotopic composition, and heavy Cu isotope was readily oxidized and preferentially released into solution (Rodríguez et al. 2015; Lv et al. 2016; Wang et al. 2017). The difference in the Cu isotopic composition ($\delta^{65}Cu_{max}$- $\delta^{65}Cu_{min}$) was ~0.80‰ for 125–250 μm and ~0.16‰ for 63–125 μm particles, with the fine particles having a narrow range of isotopic variation among the sampling sites. Because fine particles are more easily dispersed by wind and vehicle

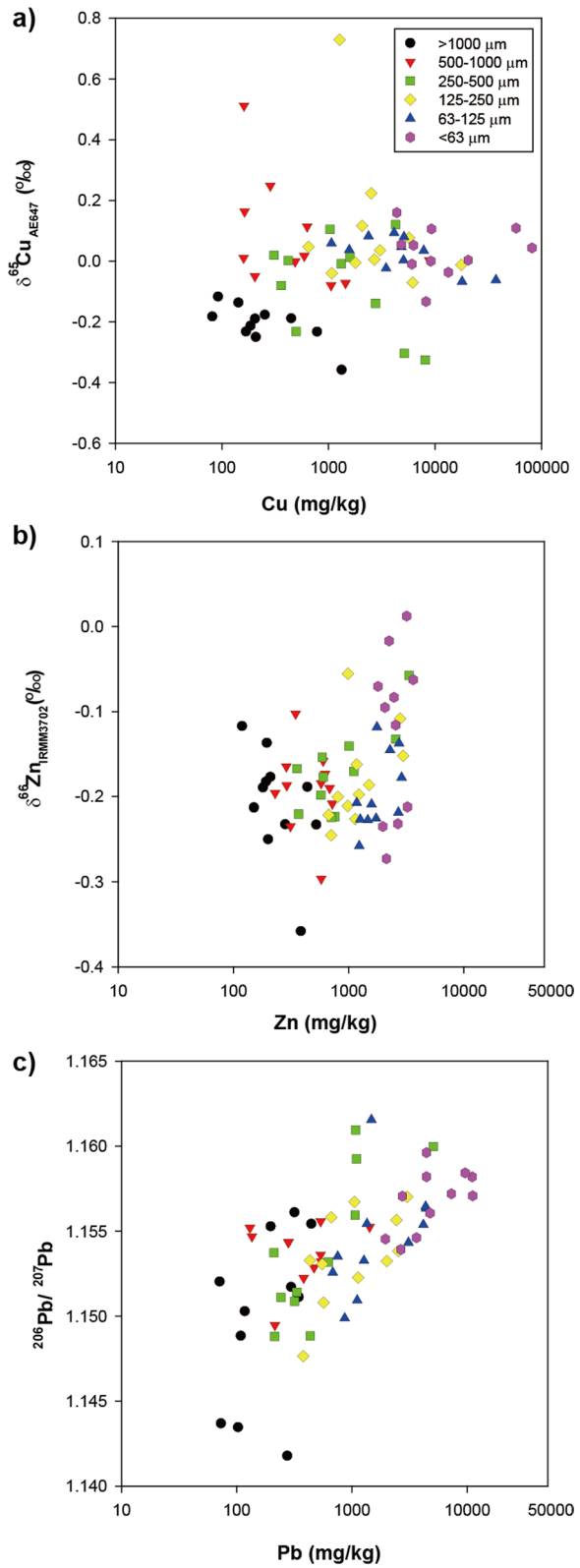

Fig. 3 Comparison of isotopic composition and concentration (mg/kg) for Cu (**a**), Zn (**b**), and Pb (**c**) in the different particle sizes of RDS samples of this study

movement than coarse particles and these concentrations are very high, the isotopic variations are likely to be small. The Cu concentrations of < 250 μm particles were high at sites 10 and 11, where small-scale, nonferrous metal processing, polishing, and manufacturing facilities are concentrated. The mean $\delta^{65}Cu_{AE647}$ of < 250 μm particles was −0.01‰, and it ranged from −0.07‰ to 0.11‰ at sites 10 and 11. Copper product (e.g., rod, billet, slab, etc.) manufacturers are located around site 4. Particles larger than 500 μm had a relatively low Cu concentration, but the Cu isotopic values were relatively high, with a mean of +0.30‰ (125–250 μm: Cu 1270 mg/kg, $\delta^{65}Cu_{AE647}$ +0.73‰; 500–1000 μm: Cu 161 mg/kg, $\delta^{65}Cu_{AE647}$ +0.51‰) (Fig. 3a).

Figure 4 presents a comparison of the Cu isotopic compositions in this study and those from the literature related to road dust and non-exhaust emissions (e.g., road paint, brake pads, and tires). The Cu isotopic signatures of RDS in this study had similar values to the road dust from São Paulo, Brazil (Souto-Oliveira et al. 2018). Mean Cu isotopic ratios in this study ($\delta^{65}Cu_{AE647}$: +0.03‰) differed only slightly from those of road paint ($\delta^{65}Cu_{AE647}$: +0.03‰) and tires ($\delta^{65}Cu_{AE647}$: +0.05‰) (Fig. 4). Meanwhile, the mean $\delta^{65}Cu_{AE647}$ of brake pads was 0.24‰ (Dong et al. 2017), which was significantly different from the isotopic ratios found in this study. The $\delta^{65}Cu_{AE647}$ values of road paint and brake pads display large variations, ranging from −0.39 to +0.35‰ (N = 3) and +0.07 to +0.42‰ (N = 3), respectively (Dong et al. 2017). The $\delta^{65}Cu_{AE647}$ of brake-derived particles was −0.03 ± 0.14‰ (N = 19, 2 s, Gonzalez et al. 2016). A previous study reported $\delta^{65}Cu_{AE647}$ values of sludge (+0.60‰), solid waste (−0.05‰), and fly ash (−0.10‰) (Bigalke et al. 2010). Cu isotopes of RDS in this study showed a wide range and there was no significant difference from that of brake-derived particles, solid waste, and fly ash (Gonzalez et al. 2016; Bigalke et al. 2010). Additionally, the Cu concentrations in this study were extremely high compared to RDS in urban areas (151 mg/kg), and those of tires (37 mg/kg) and brake pads (12 mg/kg) (Dong et al. 2017; Souto-Oliveira et al. 2018). Our results indicate that the Cu contamination of RDS seems to be more affected by Cu-related industries than by traffic activities.

Zn isotopic compositions of different RDS size fractions

The overall variation of $\delta^{66}Zn_{IRMM3702}$ in this study was ~ 0.37‰, and ranged from −0.36‰ to +0.01‰ (Table 2). The variation in $\delta^{66}Zn_{IRMM3702}$ was less than that of $\delta^{65}Cu_{NIST976}$ (~ 1.05‰), and the mean $\delta^{66}Zn_{IRMM3702}$ values of RDS were −0.21‰ (> 1000 μm), −0.19‰ (500–1000 μm), −0.17‰ (250–500 μm), −0.18‰ (125–250 μm), −0.20‰ (63–125 μm), and −0.13‰ (< 63 μm) (Table 2). Figure 3b shows a comparison between the $\delta^{66}Zn_{IRMM3702}$ and Zn concentration in the different RDS size fractions. The Zn isotopic values ($\delta^{66}Zn_{IRMM3702}$) tended to increase in smaller particle sizes. The differences of the Zn isotopic compositions ($\delta^{66}Zn_{max}$- $\delta^{66}Zn_{min}$) in the 63–125 μm fraction displayed a narrow range (~ 0.14‰), while the < 63 μm fraction showed a wide range (~ 0.29‰) compared to other particle sizes.

The mean Zn concentration in this study was slightly higher than that found in the RDS of urban areas (337 mg/kg) and brake pads (28 mg/kg), but lower than that of tires (9500 mg/kg) (Dong et al. 2017;

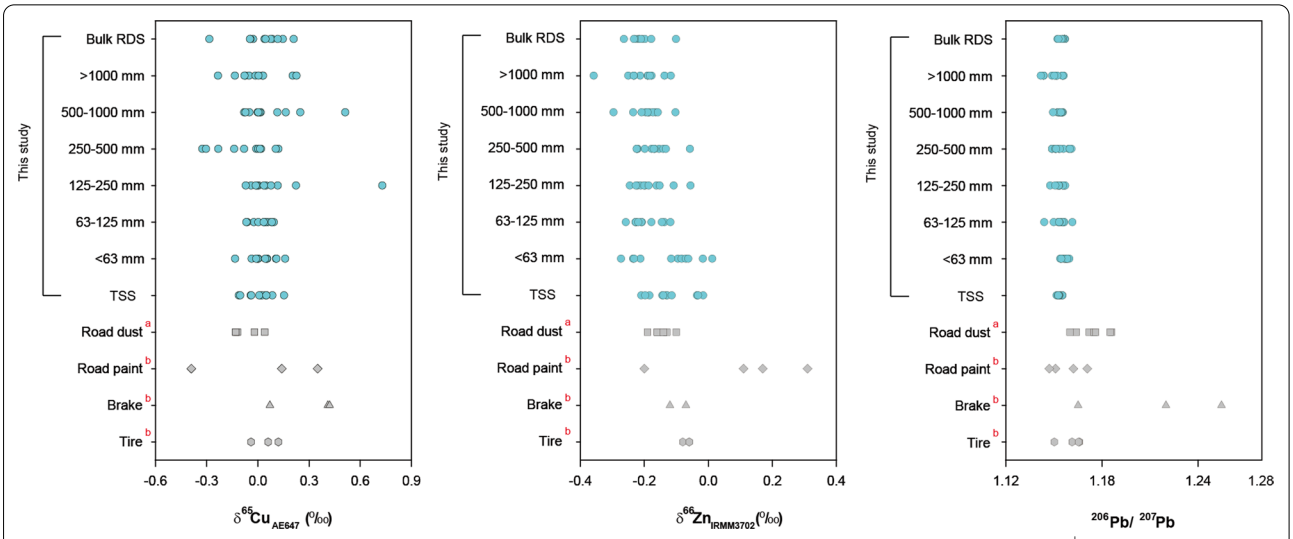

Fig. 4 Comparison of Cu, Zn, and Pb isotopic composition in this study and other literature data ([a]Souto-Oliveira et al. 2018; [b]Dong et al. 2017)

Souto-Oliveira et al. 2018). Tires contain a high Zn concentration of 8700 mg/kg (Klöckner et al. 2019). Therefore, Zn contamination of RDS caused by tire wear is widely regarded as a major source of Zn pollution in urban areas. Baensch-Baltruschat et al. (2020) reported that the tire and road wear particles generated on roads during driving of vehicles can contribute to airborne non-exhaust emissions and the average global value of tire wear emissions is about 0.8 kg/capita ranging from 0.2 to 5.5 kg. The abrasion processes increase the density of tire and road wear particles on the road surface from 1.5 to 2.2 g/cm3 (Kayhanian et al. 2012; Klöckner et al. 2019). In industrial areas, heavy-duty vehicles are used to transport raw materials and final products, so tire wear will be more severe than in urban areas. Therefore, Zn contamination in RDS derived from tire wear in industrial areas is higher than in urban areas.

Additionally, galvanized steel sheets have excellent corrosion resistance and are widely used in the automobile, steel, and metal industries, as well as for the exterior panels of facilities across South Korea. Zinc contamination has also been reported in the RDS of industrial areas in the country (Jeong et al. 2020f, g).

The mean $\delta^{66}Zn_{IRMM3702}$ of RDS from São Paulo was −0.15‰ (Souto-Oliveira et al. 2018), which was similar to the range of −0.13‰ (< 63 μm) to −0.21‰ (> 1000 μm) in this study (Fig. 4). Zinc isotopic compositions in road paints ranged from −0.20 to +0.31‰, with a mean of +0.10‰ (Dong et al. 2017). Even considering the large variability of Zn isotopic compositions, the $\delta^{66}Zn_{IRMM3702}$ in road paints was heavier than the mean RDS in urban (Souto-Oliveira et al. 2018) and industrial areas (this study). The Zn isotopic compositions in brake pads (−0.10 ‰) and tires (−0.07 ‰) were found to be within the range of RDS in urban and industrial areas (Table 2). Light Zn isotope was associated with high-temperature industrial activity, and negative Zn isotope values have been reported in the vicinity of the metallurgical industry in Barcelona (Gonzalez et al. 2016). A previous study has reported $\delta^{66}Zn_{IRMM3702}$ values of sludge (−0.71‰), solid waste (+0.30‰), and fly ash (−0.36‰) (Bigalke et al. 2010). Zn isotopic composition of RDS in this study was similar to PM_{10} in Barcelona, however, different from sludge, solid, and fly ash (Gonzalez et al. 2016; Bigalke et al. 2010).

In this study, Zn contamination of RDS was not significant when compared to Cu, and there were small Zn isotopic variations among the sampling sites and different particle sizes. Therefore, our results indicate that Zn contamination may be influenced by the traffic activities of large vehicles related to the transportation of raw materials and products, as well as to industrial activities, such as the use of galvanized steel and Cu-alloy brass containing Zn in the metal manufacturing and processing facilities at the study sites.

Pb isotopic compositions of different RDS size fractions

The $^{206}Pb/^{207}Pb$ ratio in all RDS samples ranged from 1.1418 to 1.1616, with the mean of 1.1538 (Table 2). A wide variation (0.0143) in the Pb isotopic composition ($^{206}Pb/^{207}Pb$) was observed in the > 1000 μm RDS fraction, and a narrow variation (0.0057) was found in the < 63 μm fraction. The Pb isotopic composition ($^{206}Pb/^{207}Pb$) tended to increase as the RDS particle size decreased.

Lead has been widely used in various industries, in addition to battery plates, paint additives, cable covers, and anti-corrosion materials (van der Kuijp et al. 2013; Yang et al. 2020). It is generally contained in paint additives as a stabilizer to increase their durability and moisture resistance (Apanpa-Qasim et al. 2016; Hall and Tinklenberg 2003). Megertu and Bayissa (2020) reported that extremely high Pb concentrations were found in paint samples ranging from 41 to 51,204 mg/kg. Another application for the use of Pb is the cable industry, wherein polyvinyl chloride-coated wires and cables for electrical use are stabilized with Pb. Electrical cables have been reported to contain 9518 mg/kg of Pb (Balaram et al. 2018). Copper alloys, such as brass and bronze, contain several mass percentages of Pb and are widely used in pipes due to their excellent corrosion resistance and machinability (Nakano et al. 2005). Pb concentrations showed the highest values at sampling site 4 (< 125 μm), site 6 (> 1000 μm and 500–1000 μm) site 7 (125–250 μm), and site 8 (250–500 μm), where many printing-related industries exist. Especially, for both particle sizes of < 63 μm (11,169 mg/kg) and 63–125 μm (4409 mg/kg), the highest Pb concentrations were observed at site 4 and the $^{206}Pb/^{207}Pb$ ratio was also higher than other sampling sites.

As shown in Table 2 and Fig. 4, the mean $^{206}Pb/^{207}Pb$ ratio in this study was slightly lower than that of the RDS in urban São Paulo (Souto-Oliveira et al. 2018). Differences were also observed in the mean Pb isotopic values ($^{206}Pb/^{207}Pb$) relative to road paints, brake pads, and tires, which are affected by traffic activities (Dong et al. 2017). The mean Pb concentration in the industrial area was extremely high when compared to RDS in urban areas (37 mg/kg), tires (11 mg/kg), and brake pads (16 mg/kg; Dong et al. 2017, Souto-Oliveira et al. 2018). Although there are no Pb isotope data expected as a potential of Pb contamination source in this study, our results showed that Pb contamination in RDS was found to be mainly affected by industrial activities (e.g., many printings, wire manufacturing, and Cu-related manufacturing and processing) rather than traffic activity. To more clearly

identify potential sources of RDS contamination in industrial areas, it is necessary to establish isotopic data for raw materials and final products of the study area.

Relationship between different RDS size fractions and TSS in runoff

Generally, RDS on the road surface exists as a mixture of various particle sizes. Sutherland (2003) reported that the most important index of RDS pollution is the mass loading of heavy metals in each grain size fraction. Grain size mass partitioning revealed that the 250–500-μm fraction was dominant, and accounted for 22.4% of the RDS samples (Fig. 5). Although the finest fraction (< 63 μm) accounted for 17.1% of total RDS as a mass fraction, the amounts of metal accumulated in the fines fraction (< 63 μm) of RDS were higher than other RDS sizes. The mean of metal loading of this fraction accounted for 40.0% of Cr, 45.4% of Ni, 56.3% of Cu, 33.9% of Zn, 32.4% of As, 50.2% of Cd, and 54.3% of Pb in the total RDS.

The mobility of RDS on the road surface during rainfall events strongly depends on particle size. Fine particle fractions are easily transported by rainfall, which is important because the concentrations and $GSF_{loading}$ of metals are higher in smaller particles in urban and industrial regions (Lanzerstorfer 2020; Sutherland 2003; Jeong et al. 2020d; Zhao et al. 2010). Indeed, the fine particles (< 63 μm) had higher Cu, Zn, and Pb concentrations and isotopic values than the coarser fractions (Fig. 3).

The mean concentration of Cu in TSS was 16,294 mg/kg, which was similar to that observed in the < 63 μm RDS (20,089 mg/kg) (Table 1). Moreover, the Cu isotopic composition of TSS varied between −0.11 and +0.15 ‰ (mean $\delta^{65}Cu_{AE647}$: +0.01‰), which was within the range of RDS (Table 2, Fig. 4). A higher concentration of Cu was observed in the < 63 μm fraction in RDS than in the TSS, but a 3.9 times higher concentration of Zn was found in the TSS (9921 mg/kg) than in the < 63 μm fraction in RDS (2541 mg/kg). The mean Zn isotopic value ($\delta^{66}Zn_{IRMM3702}$) was −0.11‰ and ranged from −0.21 to −0.02‰; similar to the Cu isotopes, the Zn isotopic ratio of the TSS was also the most similar value to the < 63 μm RDS fraction (mean $\delta^{66}Zn_{IRMM3702}$: −0.13‰) (Table 2). The mean Pb concentration in the < 63 μm fraction of RDS (5797 mg/kg) was higher than that of the TSS (2391 mg/kg), in the latter of which the mean $^{206}Pb/^{207}Pb$ value was 1.1534. The Pb isotopic compositions showed less variability in the TSS than in all RDS size fractions (Fig. 4).

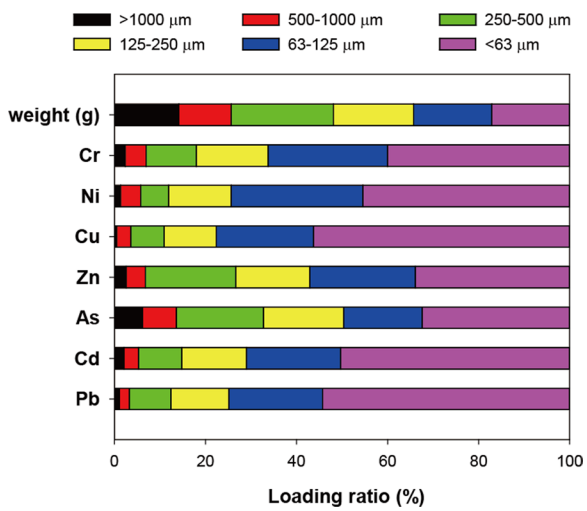

Fig. 5 Heavy metal loading percentage (%) of six different particle sizes in RDS

A hierarchical cluster analysis was conducted to examine the relationships between different sizes of RDS and TSS (Fig. 6). The clustering procedure generated two groups—Group 1, which included the 125–250, 250–500, 500–1000, and > 1000 μm RDS, and Group 2, which included the < 63 μm in RDS and TSS. These results indicate that the finest RDS and TSS were correlated. Brodie and Dunn (2009) investigated stormwater monitoring with different rainfall events and reported that the runoff particle size distribution was dominated by particles < 63 μm. Our results show that the Cu, Zn, and Pb isotopic values of the TSS were closely related to the < 63 μm RDS fraction.

Research on rainfall runoff has been conducted focusing on fine particle size fractions. However, different size fractions, such as < 38 μm (Kayhanian et al. 2012), < 44 μm (Zhao et al. 2010), < 63 μm (Camponelli et al. 2010), < 75 μm (Li and Zuo 2013), < 125 μm (Jeong et al. 2020d), and < 250 μm (Aryal et al. 2017), have been proposed for different regions and by different researchers. In our previous study, we reported that when the total rainfall was 74 mm and the mean rainfall intensity was 7 mm/h, the < 125 μm fraction accounted for 53.9–98.7% (Jeong et al. 2020d). This difference may have been affected by various environmental conditions, such as rainfall intensity, antecedent dry period, and land use type. In this study, TSS data were collected when precipitation was low; hence, fine particles were preferentially discharged, and the TSS showed much higher metal concentrations than the < 63 μm RDS. The total amount of rainfall in the study area in 2018 was 1135 mm, and there were 95 annual precipitation days. The number of days with a daily rainfall of < 10 mm was 67 days, accounting for 70% of all annual precipitation days. Recently, Lanzerstorfer (2020) suggested that 63 μm would be the upper size limit for runoff studies. Our results also indicate that small particles (< 63 μm) are more suitable for tracing pollution sources than

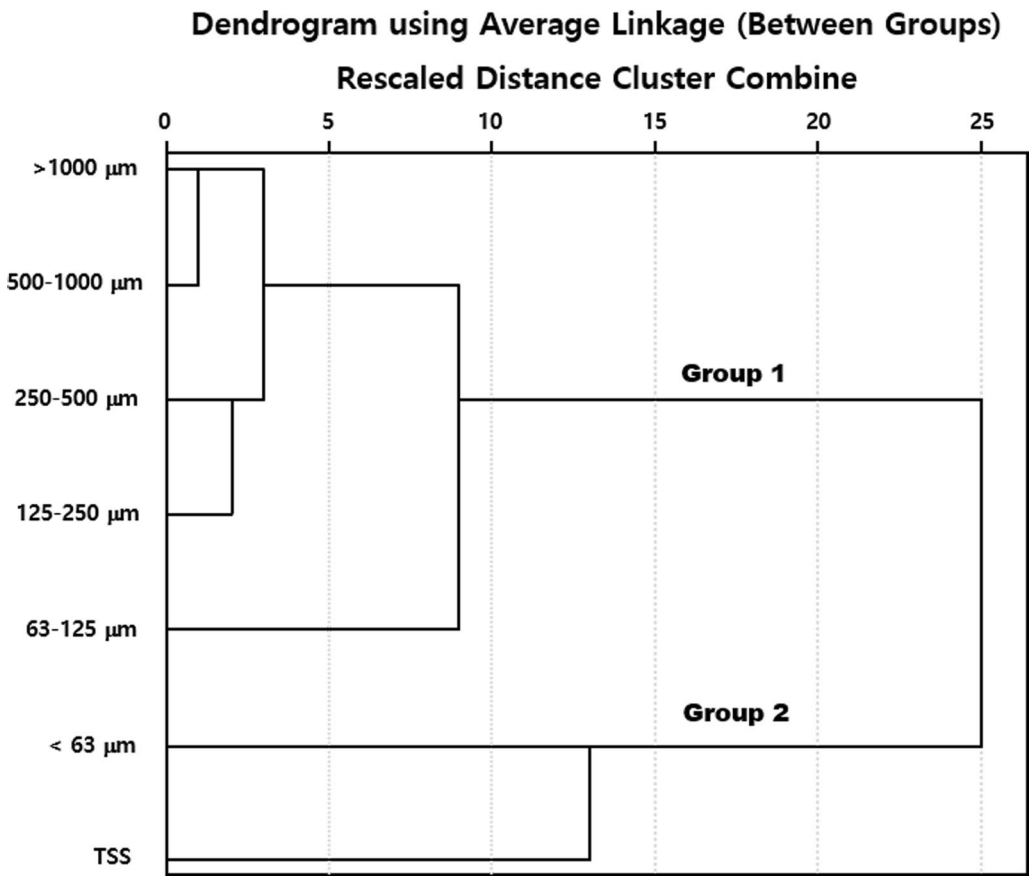

Fig. 6 Dendrogram showing clustering of the TSS in runoff and six different particle sizes of RDS in this study

larger ones in runoff studies using a Cu, Zn, and Pb multi-isotope approach.

Application of multi-isotopes as a useful tool for source identification in RDS studies

Studies on the concentrations and elemental ratios of heavy metals in urban RDS are still used to assess metal pollution levels and their adverse effects on surrounding environments and human health (e.g., Bian et al. 2015; Hwang et al. 2016; Roy et al. 2019). However, this approach is limited in its utility for determining the specific sources of contamination and discriminating among them. Figure 7 shows the bivariate, multi-isotope plots produced in this study and from existing data in the literature, including Cu, Zn, and Pb isotopic compositions. Because we divided the RDS samples into six different size fractions, the variations in the Cu and Zn isotopic compositions were large. The combination of Cu and Zn isotopes could not be used to distinguish between urban road dust (Souto-Oliveira et al. 2018) and industrial RDS (this study) (Fig. 7a). Road dust in São Paulo seems to be distinct from brake pad and tire wear (Dong et al. 2017), yet the RDS data in this study could not be differentiated due to differences in the isotopic values by land use type and country (Fig. 7a). This may be due to the lack of data and differences between countries and/or manufacturers.

Figure 7b shows the relationship between the Cu and Pb isotopic compositions in this study and previously reported values. Our results suggest that the combination of Pb and Cu isotopes provides better information than that of Cu and Zn isotopes for the purpose of differentiating among pollution sources and urban and industrial RDS. No difference was observed between the urban road dust and industrial RDS in this study using Zn isotopes alone, but the combination of Pb and Zn isotopes yielded clearly differentiated isotopic values (Fig. 7c). Meanwhile, the Pb and Zn isotopes in brake pads and tires, which are major causes of metal contamination from traffic activities, displayed different characteristics from industrial RDS and urban road dust (Dong et al. 2017; Souto-Oliveira et al. 2018).

Isotopic data for road dust, road paint, brake pads, and tires related to traffic activities have been limited so far, and Cu, Zn, and Pb isotopic values may be influenced

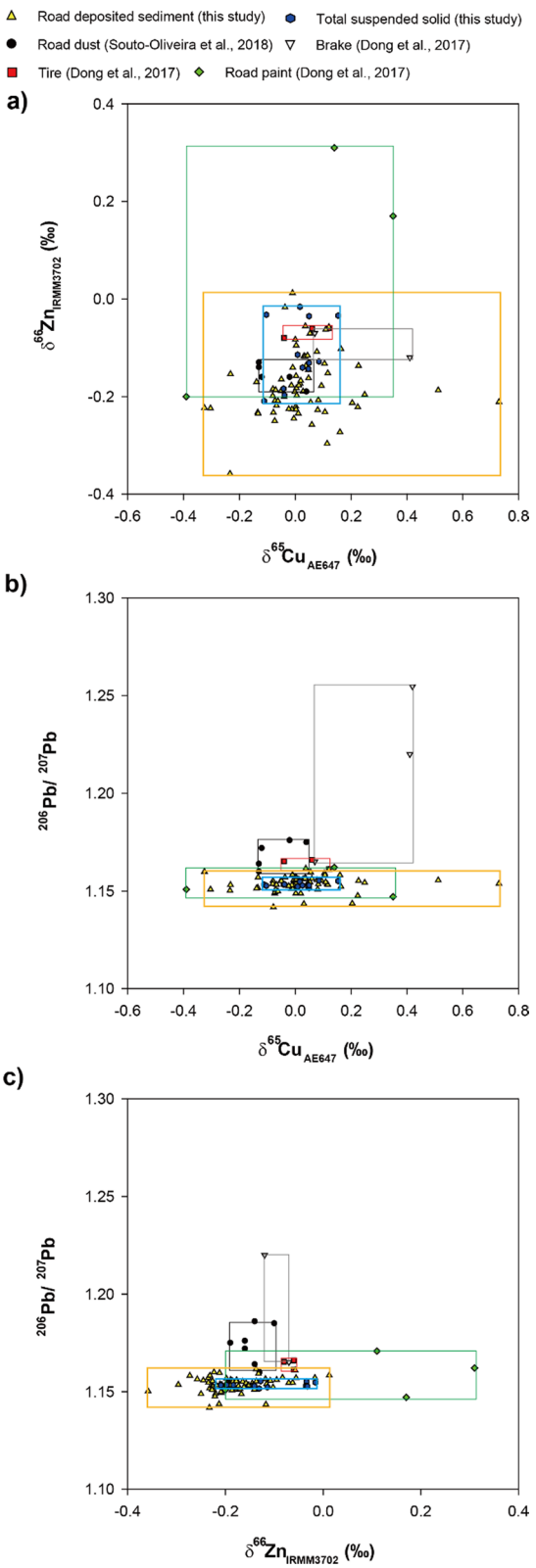

Fig. 7 Multi-isotope diagrams of this study and other literature data using $\delta^{65}Cu_{AE647}$ vs $\delta^{66}Zn_{IRMM3702}$ (**a**), $\delta^{65}Cu_{AE647}$ vs $^{206}Pb/^{207}Pb$ (**b**) and $\delta^{66}Zn_{IRMM3702}$ vs $^{206}Pb/^{207}Pb$ (**c**)

by natural and anthropogenic factors, depending upon the region. The application of a multi-isotope approach using Cu, Zn, and Pb as environmental tracers may be key to identifying potential sources of metal pollution, as well as for understanding the environmental pollution and contribution of RDS in various environments, especially urban and industrial areas. However, the Cu, Zn, and Pb isotopic compositions in various environments are still poorly reported. In this study, the combination of a Pb and either Cu or Zn isotopic signature revealed the differences among road paints, brake pads, and tires. Multi-isotope (Cu, Zn, and Pb) data on a variety of anthropogenic pollutants from different countries and manufacturers are necessary, and the establishment of a database on multi-isotope values would greatly contribute to the identification and management of individual sources of metal pollution.

Conclusions

We evaluated a multi-isotope (Cu, Zn, and Pb) signature for the purpose of characterizing the differences in the isotopic values of different RDS sizes fractions and to understand the relationship between RDS and TSS in runoff from industrial areas in Korea. The Cu concentration in RDS was highest when compared to other metal elements due to the influence of industrial copper smelting/refining facilities and adjacent Cu-related industries. There was a wide variation in $\delta^{65}Cu_{AE647}$ of ~ 1.05‰ and no correlation was observed between Cu isotope and concentration values. The Cu isotopes of RDS around a copper smelting facility were different from those of Cu-related metal processing facilities. Meanwhile, Zn isotopic compositions showed less variation (~ 0.37‰) than Cu, and the $\delta^{66}Zn_{IRMM3702}$ and $^{206}Pb/^{207}Pb$ ratios tended to increase in the smaller RDS particle sizes. The combination of Pb and either Cu or Zn isotopic signatures revealed the differences in road paint, brake pad, and tire from traffic activities. The Cu, Zn, and Pb isotopic compositions of TSS in runoff were closely related to the fine RDS particle sizes (< 63 μm) in this study, suggesting that small particles are more suitable for tracing pollution sources than large particles in runoff studies using a multi-isotope (Cu, Zn, and Pb) approach. We also proposed for the first time that multi-isotopes (Cu, Zn, and Pb) in the RDS studies of industrial areas could serve as valuable tracers for the identification and discrimination of sources of metal pollution. To gain a more accurate understanding and improve the source identification of metal pollution processes, further investigation and more isotopic information from a variety of potential sources by natural, industrial, and traffic activities are needed. The application of multi-isotope (Cu, Zn, and Pb) approaches will contribute to the identification and

management of individual sources of metal pollution in urban environments.

Acknowledgements
We thank Jihyun Lee and Seung-yong Lee for helping us with RDS and TSS sampling.

Authors' contributions
HJ was involved in conceptualization, methodology, visualization, writing—original draft. KR helped in methodology, investigation, writing—review & editing, funding acquisition. Both authors read and approved the final manuscript.

Funding
This work was supported by the Korea Institute of Ocean Science and Technology (Grant No. PE 99912).

Availability of data and materials
All data for this study are available from the corresponding author on request.

Declarations

Competing interests
The authors declare no competing interests in relation to the work described.

Author details
[1]Marine Environmental Research Center, Korea Institute of Ocean Science and Technology (KIOST), Busan 49111, Republic of Korea. [2]Department of Ocean Science (Oceanography), KIOST School, University of Science and Technology (UST), Daejeon 34113, Republic of Korea.

Received: 28 April 2021 Accepted: 10 August 2021
Published online: 20 August 2021

References

Adamiec E, Jarosz-Krzeminska E, Wiezala R. Heavy metals from non-exhaust vehicle emissions in urban and motorway road dusts. Environ Monit Assess. 2016;188:369. https://doi.org/10.1007/s10661-016-5377-1.

Amato F, Pandolfi M, Viana M, Querol X, Alastuey A, Moreno T. Spatial and chemical patterns of PM_{10} in road dust deposited in urban environment. Atmos Environ. 2009;43:1650–9. https://doi.org/10.1016/j.atmosenv.2008.12.009.

Amato F, Viana M, Richard A, Furger M, Prévôt ASH, Nava S, Lucarelli F, Bukowiecki N, Alastuey A, Reche C, Moreno T, Pandolfi M, Pey J, Querol X. Size and time-resolved roadside enrichment of atmospheric particulate pollutants. Atmos Chem Phys. 2011;1:2917–31. https://doi.org/10.5194/acp-11-2917-2011.

Amato F, Schaap M, Denier van der Gon HAC, Pandolfi M, Alastuey A, Keuken M, Querol X. Effect of rain events on the mobility of road dust load in two dutch and Spanish roads. Atmos Environ. 2012;62:352–8. https://doi.org/10.1016/j.atmosenv.2012.08.042.

Apanpa-Qasim AFI, Adeyi AA, Mudliar SN, Raghunathan KR, Thawale P. Examination of lead and cadmium in water-based paints marketed in Nigeria. J Health Pollut. 2016;6:43–9. https://doi.org/10.5696/2156-9614-6.12.43.

Araújo DF, Boaventura GR, Viers J, Mulholland DS, Weiss D, Araujo D, Lima B, Ruiz I, Machado W, Babinski M, Dantas E. Ion exchange chromatography and mass bias correction for accurate and precise Zn isotope ratio measurements in environmental reference materials by MC-ICP-MS. J Braz Chem Soc. 2017;28:225–35. https://doi.org/10.5935/0103-5053.20160167.

Araújo DF, Ponzevera E, Briant N, Knoery J, Sireau T, Mojtahid M, Metzger E, Branch-Papa C. Assessment of the metal contamination evolution in the Loire estuary using Cu and Zn stable isotopes and geochemical data in sediments. Mar Pollut Bull. 2019a;143:12–23. https://doi.org/10.1016/j.marpolbul.2019.04.034.

Araújo DF, Ponzevera E, Briant N, Knoery J, Bruzac S, Sireau T, Brach-Papa C. Copper, zinc and lead isotope signatures of sediments from a Mediterranean coastal bay impacted by naval activities and urban sources. Appl Geochem. 2019b;111: 104440. https://doi.org/10.1016/j.apgeochem.2019.104440.

Aryal R, Beecham S, Sarkar B, Chong MN, Kinsela A, Kandasamy J, Vigneswaran S. Readily wash-off road dust and associated heavy metals on motorways. Water Air Soil Pollut. 2017;228:1. https://doi.org/10.1007/s11270-016-3178-3.

Baensch-Baltruschat B, Kocher B, Stock F, Reifferscheid G. Tyre and road wear particles (TRWP)—a review of generation, properties, emissions, human health risk, ecotoxicity, and fate in the environment. Sci Total Environ. 2020;733: 137823. https://doi.org/10.1016/j.scitotenv.2020.137823.

Balaram V, Rambabu U, Reddy MRP, Muniranthanam NR, Chatterjee S. RoHS Regulation: challenges in the measurement of substances of concern in industrial products by different analytical techniques. Mapan. 2018;33:329–46. https://doi.org/10.1007/s12647-018-0263-7.

Bian B, Lin C, Wu HS. Contamination and risk assessment of metals in road-deposited sediments in a medium-sized city of China. Ecotoxicol Environ Safe. 2015;112:87–95. https://doi.org/10.1016/j.ecoenv.2014.10.030.

Bigalke M, Weyer S, Kobza J, Wilcke W. Stable Cu and Zn isotope ratios as tracers of sources and transport of Cu and Zn in contaminated soil. Geochim Cosmochim Acta. 2010;74:6801–13. https://doi.org/10.1016/j.gca.2010.08.044.

Bourotte CLM, Sugauara LE, De Marchi MRR, Souto-Oliveira CE. Trace metal and PAHs in topsoils of the university campus in the megacity of Sao Paulo, Brazil. An Acad Bras Ciênc. 2019;91: e20180334. https://doi.org/10.1590/0001-3765201920180334.

Bretón JGC, Bretón RMC, Guzman AAE, Guarnaccia C, Morales SM, Severino RCL, Marrón MR, López GH, Lozada SEC, Kahl JDW, Pech IEP, Lara ER, Fuentes MLE. Trace metal content and health risk assessment of PM_{10} in an urban environment of León, Mexico. Atmosphere. 2019;10:573. https://doi.org/10.3390/atmos10100573.

Brodie I, Dunn P. Suspended particle characteristics in storm runoff from urban impervious surfaces in Toowoomba, Australia. Urban Water J. 2009;6:137–46. https://doi.org/10.1080/15730620802541607.

Camponelli KM, Lev SM, Snodgrass JW, Landa ER, Casey RE. Chemical fractionation of Cu and Zn in stormwater, roadway dust and stormwater pond sediments. Environ Pollut. 2010;158:2143–9. https://doi.org/10.1016/j.envpol.2010.02.024.

Desaulty AM, Perret S, Maubec N, Négrel P. Tracking anthropogenic sources in a small catchment using Zn-isotope signatures. Appl Geochem. 2020;123: 104788. https://doi.org/10.1016/j.apgeochem.2020.104788.

Dong S, Gonzalez RO, Harrison RM, Green D, North R, Fowler G, Weiss D. Isotopic signatures suggest important contributions from recycled gasoline, road dust and non-exhaust traffic sources for copper, zinc and lead in PM10 in London, United Kingdom. Atmos Environ. 2017;165:88–98. https://doi.org/10.1016/j.atmosenv.2017.06.020

Gmochowska W, Pietranik A, Tyszka R, Ettler V, Mihaljevič M, Długosz M, Walenczak K. Sources of pollution and distribution of Pb, Cd and Hg in Wrocław soils: Insight from chemical and Pb isotope composition. Geochemistry. 2019;79:434–45. https://doi.org/10.1016/j.chemer.2019.07.002.

Gonzalez RO, Strekopytov S, Amato F, Querol X, Reche C, Weiss D. New insights from Zinc and Copper isotopic compositions into the sources of atmospheric particulate matter from two major European Cities. Environ Sci Technol. 2016;50:9816–24. https://doi.org/10.1021/acs.est.6b00863.

Graney JR, Edgerton ES, Landis MS. Using Pb isotope ratios of particulate matter and epiphytic lichens from the Athabasca Oil Sands Region in Alberta, Canada to quantify local, regional, and global Pb source contributions. Sci Total Environ. 2019;654:1293–304. https://doi.org/10.1016/j.scitotenv.2018.11.047.

Hall GS, Tinklenberg J. Determination of Ti, Zn, and Pb in lead-based house paints by EDXRF. J Anal Atomic Spectrom. 2003;18:775–8. https://doi.org/10.1039/B300597F.

Hwang HM, Fiala MJ, Park D, Wade TL. Review of pollutants in urban road dust and stormwater runoff: part 1. Heavy metals released from vehicles. Int J Urban Sci. 2016;20:334–60. https://doi.org/10.1080/12265934.2016.1193041.

Iijima A, Sato K, Yano K, Tago H, Kato M, Kimura H, Furuta N. Particle size and composition distribution analysis of automotive brake abrasion dusts for the evaluation of antimony sources of airborne particulate matter. Atmos Environ. 2007;41:4908–19. https://doi.org/10.1016/j.atmosenv.2007.02.005.

Jeong J, Lee J, Choi JY, Kim KT, Kim ES, Ra K. Assessment of contamination and sources identification of heavy metals in stream water and sediments around industrial complex. Kor J Ecol Environ. 2019;52:179–91. https://doi.org/10.11614/KSL.2019.52.3.179.

Jeong H, Choi JY, Lim J, Shim WJ, Kim YO, Ra K. Characterization of the contribution of road deposited sediments to the contamination of the close marine environment with trace metals: Case of the port city of Busan (South Korea). Mar Pollut Bull. 2020a;161: 111717. https://doi.org/10.1016/j.marpolbul.2020.111717.

Jeong H, Choi JY, Lee J, Ra K. Investigation of Pb and Cu isotopes to trace contamination sources from the Artificial Shihwa Lake in Korea. J Coast Res. 2020b;SI95:1122–7. https://doi.org/10.2112/SI95-218.1.

Jeong H, Choi JY, Lim J, Ra K. Pollution caused by potentially toxic elements present in road dust from industrial areas in Korea. Atmosphere. 2020c;11:1366. https://doi.org/10.3390/atmos11121366.

Jeong H, Choi JY, Lee J, Lim J, Ra K. Heavy metal pollution by road-deposited sediments and its contribution to total suspended solids in rainfall runoff from intensive industrial areas. Environ Pollut. 2020d;265: 115028. https://doi.org/10.1016/j.envpol.2020.115028.

Jeong H, Choi JY, Ra K. Study on heavy metal pollution sources to Shihwa Lake: characteristics of heavy metal in size-fractionated road dust from urban area and the impacts to marine environments. J Korean Soc Mar Environ Energy. 2020e;23:70–80. https://doi.org/10.7846/JKOSMEE.2020.23.2.70.

Jeong H, Choi JY, Ra K. Assessment of metal pollution of road-deposited sediments and marine sediments around Gwangyang Bay. Korea J Korean Soc Oceanogr. 2020f;25:42–53. https://doi.org/10.7850/jkso.2020.25.2.042.

Jeong H, Choi JY, Ra K. Characteristics for heavy metal pollution in road dust from Daebul industrial complex: classification by particle size and magnetic separation. J Environ Impact Assess. 2020g;29:252–71. https://doi.org/10.14249/eia.2020.29.4.252.

Jeong H, Ra K, Choi JY. Cu, Zn, and Pb isotopic compositions of various geological and biological reference materials. Geostand Geoanal Res. 2021. https://doi.org/10.1111/ggr.12379.

Kayhanian M, McKenzie ER, Leatherbarrow JE, Young TM. Characteristics of road sediment fractionated particles captured from paved surfaces, surface run-off and detention basins. Sci Total Environ. 2012;439:172–86. https://doi.org/10.1016/j.scitotenv.2012.08.077.

Khalid N, Hussain M, Young HS, Boyce B, Aqeel M, Noman A. Effects of road proximity on heavy metal concentrations in soils and common roadside plants in Southern California. Environ Sci Pollut Res. 2018;25:35257–65. https://doi.org/10.1007/s11356-018-3218-1.

Klöckner P, Reemtsma T, Eisentraut P, Braun U, Ryhl AS, Wagner S. Tire and road wear particles in road environment-Quantification and assessment of particle dynamics by Zn determination after density separation. Chemosphere. 2019;222:714–21. https://doi.org/10.1016/j.chemosphere.2019.01.176.

Konečný L, Ettler V, Kristiansen SM, Amorim MJB, Kříbek B, Mihaljevič M, Šebek O, Nyambe I, Scott-Fordsmand JJ. Response of *Enchytraeus crypticus* worms to high metal levels in tropical soils polluted by copper smelting. J Geochem Explor. 2014;144:427–32. https://doi.org/10.1016/j.gexplo.2013.10.004.

Lanzerstorfer C. Toward more intercomparable road dust studies. Crit Rev Environ Sci Technol. 2020. https://doi.org/10.1080/10643389.2020.1737472.

Li H, Zuo XJ. Speciation and size distribution of copper and zinc in urban road runoff. Bull Environ Contam Toxicol. 2013;90:471–6. https://doi.org/10.1007/s00128-012-0953-8.

Li Y, Shen Y, Pi L, Hu W, Chen M, Luo Y, Li Z, Su S, Ding S, Gan Z. Particle size distribution and perchlorate levels in settled dust from urban roads, parks, and roofs in Chengdu, China. Environ Sci Processes Impacts. 2016;18:72–7. https://doi.org/10.1039/C5EM00435G.

Little SH, Vance D, McManu J, Severmann S, Lyons TW. Copper isotope signatures in modern marine sediments. Geochim Cosmochim Acta. 2017;212:253–73. https://doi.org/10.1016/j.gca.2017.06.019.

Lv Y, Liu SA, Zhu JM, Li S. Copper and zinc isotope fractionation during deposition and weathering of highly metalliferous black shales in central China. Chem Geol. 2016;445:24–35. https://doi.org/10.1016/j.chemgeo.2016.01.016.

Megertu DG, Bayissa LD. Heavy metal contents of selected commercially available oil-based house paints intended for residential use in Ethiopia. Environ Sci Pollut Res. 2020;27:17175–83. https://doi.org/10.1007/s11356-020-08297-z.

Mihaljevič M, Baieta R, Ettler V, Vaněk A, Kříbek B, Penížek V, Drahota P, Trubač J, Sracek O, Chrastný V, Mapani BS. Tracing the metal dynamics in semi-arid soils near mine tailings using stable Cu and Pb isotopes. Chem Geol. 2019;515:61–76. https://doi.org/10.1016/j.chemgeo.2019.03.026.

Mil-Homens M, Vale C, Brito P, Naughton F, Drago T, Raimundo J, Anes B, Schmidt S, Caetano M. Insights of Pb isotopic signature into the historical evolution and sources of Pb contamination in a sediment core of the southwestern Iberian Atlantic shelf. Sci Total Environ. 2017;586:473–84. https://doi.org/10.1016/j.scitotenv.2017.01.204.

Moeller K, Schoenberg R, Pedersen RB, Weiss D, Dong S. Calibration of the new certified reference materials ERM-AE633 and ERM-AE647 for copper and IRMM-3702 for zinc isotope amount ratio determinations. Geostand Geoanal Res. 2012;36:177–99. https://doi.org/10.1111/j.1751-908X.2011.00153.x.

Nakano A, Rochman NT, Sueyoshi H. Removal of lead from copper alloy scraps by compound-separation method. Mater Trans. 2005;46:2719–24. https://doi.org/10.2320/matertrans.46.2719.

Nawrot N, Wojciechowska E, Matej-Łukowicz K, Walkusz-Miotk J, Pazdro K. Spatial and vertical distribution analysis of heavy metals in urban retention tanks sediments: a case study of Strzyza Stream. Environ Geochem Health. 2020;42:1469–85. https://doi.org/10.1007/s10653-019-00439-8.

Novak M, Sipkova A, Chrastny V, Stepanova M, Voldrichova P, Veselovsky F, Prechova E, Blaha V, Curik J, Farkas J, Erbanova L, Bohdalkova L, Pasava J, Mikova J, Komarek A, Krachler M. Cu-Zn isotope constraints on the provenance of air pollution in Central Europe: Using soluble and insoluble particles in snow and rime. Environ Pollut. 2016;218:1135–46. https://doi.org/10.1016/j.envpol.2016.08.067.

Popoola LT, Adebanjo SA, Adeoye BK. Assessment of atmospheric particulate matter and heavy metals: a critical review. Int J Environ Sci Technol. 2017;15:935–48. https://doi.org/10.1007/s13762-017-1454-4.

Rodríguez NP, Khoshkhoo M, Sandström Å, Rodushkin I, Alakangas L, Öhlander B. Isotopic signature of Cu and Fe during bioleaching and electrochemical leaching of a chalcopyrite concentrate. Int J Miner Process. 2015;134:58–65. https://doi.org/10.1016/j.minpro.2014.11.010.

Rosca C, Schoenberg R, Tomlinson EL, Kamber BS. Combined zinc-lead isotope and trace metal assessment of recent atmospheric pollution sources recorded in Irish peatlands. Sci Total Environ. 2019;658:234–49. https://doi.org/10.1016/j.scitotenv.2018.12.049.

Roy S, Gupta SJ, Prakash J, Habib G, Baudh K, Nasr M. Ecological and human health risk assessment of heavy metal contamination in road dust in the National Capital Territory (NCT) of Delhi. India Environ Sci Pollut Res. 2019;26:30413–25. https://doi.org/10.1007/s11356-019-06216-5.

Schleicher NJ, Dong S, Packman H, Little SH, Ochoa-González R, Najorka J, Sun Y, Weiss DJ. A global assessment of copper, zinc, and lead isotopes in mineral dust sources and aerosols. Front Earth Sci. 2020;8:167. https://doi.org/10.3389/feart.2020.00167.

Song S, Mathur R, Ruiz J, Chen D, Allin N, Guo K, Kang W. Fingerprinting two metal contaminants in stream with Cu isotopes near the Dexing Mine, China. Sci Total Environ. 2016;544:677–85. https://doi.org/10.1016/j.scitotenv.2015.11.101.

Souto-Oliveira CE, Babinski M, Araújo DF, Andrade MF. Multi-isotopic fingerprints (Pb, Zn, Cu) applied for urban aerosol source apportionment and discrimination. Sci Total Environ. 2018;626:1350–66. https://doi.org/10.1016/j.scitotenv.2018.01.192.

Souto-Oliveira CE, Babinski M, Araújo DF, Weiss DJ, Ruiz IR. Multi-isotope approach of Pb, Cu and Zn in urban aerosols and anthropogenic sources improves tracing of the atmospheric pollutant sources in megacities. Atmos Environ. 2019;198:427–37. https://doi.org/10.1016/j.atmosenv.2018.11.007.

Spinks SC, Uvarova Y. Fractionation of Zn isotopes in terrestrial ferromanganese crusts and implications for tracing isotopically-heterogeneous metal sources. Chem Geol. 2019;529: 119314. https://doi.org/10.1016/j.chemgeo.2019.119314.

Sutherland RA. Lead in grain size fractions of road-deposited sediment. Environ Pollut. 2003;121:229–37. https://doi.org/10.1016/S0269-7491(02)00219-1.

Tu YJ, You CF, Kuo TY. Source identification of Zn in Erren River, Taiwan: an application of Zn isotopes. Chemosphere. 2020;248: 126044. https://doi.org/10.1016/j.chemosphere.2020.126044.
van der Kuijp TJ, Huang L, Cherry CR. Health hazards of China's lead-acid battery industry: a review of its market drivers, production processes, and health impacts. Environ Health. 2013;12:61. https://doi.org/10.1186/1476-069X-12-61.
Wang M, Zhang H. Accumulation of heavy metals in roadside soil in urban area and the related impacting factors. Int J Environ Res Public Health. 2018;15:1064. https://doi.org/10.3390/ijerph15061064.
Wang Q, Zhou L, Little SH, Liu J, Feng L, Tong S. The geochemical behavior of Cu and its isotopes in the Yangtze River. Sci Total Environ. 2020;728: 138428. https://doi.org/10.1016/j.scitotenv.2020.138428.
Wang Z, Chen J, Zhang T. Cu isotopic composition in surface environments and in biological systems: a critical review. Int J Environ Res Public Health. 2017;14:538. https://doi.org/10.3390/ijerph14050538.
Wentworth CK. A scale of grade and class terms for clastic sediments. J Geol. 1992;30:377–92. https://doi.org/10.1086/622910.
Yang J, Li X, Xiong Z, Wang M, Liu Q. Environmental pollution effect analysis of lead compounds in China based on life cycle. Int J Environ Res Public Health. 2020;17:2184. https://doi.org/10.3390/ijerph17072184.
Zhao H, Li X, Wang X, Tian D. Grain size distribution of road-deposited sediment and its contribution to heavy metal pollution in urban runoff in Beijing, China. J Hazard Mater. 2010;183:203–10. https://doi.org/10.1016/j.jhazmat.2010.07.012.
Zafra CA, Temprano J, Tejero I. Distribution of the concentration of heavy metals associated with the sediment particles accumulated on road surface. Environ Technol. 2011;32:997–1008. https://doi.org/10.1080/09593330.2010.523436.

Publisher's Note

Springer Nature remains neutral with regard to jurisdictional claims in published maps and institutional affiliations.

Submit your manuscript to a SpringerOpen journal and benefit from:

- ► Convenient online submission
- ► Rigorous peer review
- ► Open access: articles freely available online
- ► High visibility within the field
- ► Retaining the copyright to your article

Submit your next manuscript at ► springeropen.com